atmosphere

MDPI

Article

Spatial and Temporal Trends of Gaseous Elemental Mercury over a Highly Impacted Coastal Environment (Northern Adriatic, Italy)

Nicolò Barago [1], Federico Floreani [1,2], Alessandro Acquavita [3,*], José María Esbrí [4], Stefano Covelli [1] and Pablo Higueras [4]

1 Department of Mathematics & Geoscience, University of Trieste, Via Weiss 2, 34128 Trieste, Italy; NICOLO.BARAGO@phd.units.it (N.B.); FEDERICO.FLOREANI@phd.units.it (F.F.); covelli@units.it (S.C.)
2 Department of Life Sciences, University of Trieste, Via Giorgieri 5, 34127 Trieste, Italy
3 ARPA FVG Regional Agency for Environmental Protection of Friuli Venezia Giulia, Via Cairoli 14, Palmanova, 33057 Udine, Italy
4 Institute of Applied Geology, Heavy Metals Biogeochemistry Laboratory, University of Castilla-La Mancha, Plaza Manuel Meca, 13400 Almaden, Spain; JoseMaria.Esbri@uclm.es (J.M.E.); Pablo.Higueras@uclm.es (P.H.)
* Correspondence: alessandro.acquavita@arpa.fvg.it; Tel.: +39-0432-191-8230

Received: 1 August 2020; Accepted: 27 August 2020; Published: 31 August 2020

Abstract: Mercury (Hg) is a global pollutant, being highly persistent in the atmosphere, in particular gaseous elemental mercury (GEM), which can easily be emitted and then transported over long distances. In the Gulf of Trieste (northern Adriatic Sea, Italy), contamination by Hg is well characterised but little is known regarding the concentrations, sources and fate of GEM in the atmosphere. In this work, discrete measurements of GEM were recorded from several sites at different times of the year. The database is consistent with temporal night-day variations monitored using a continuous real-time device. The meteorological conditions were collected as ancillary parameters. GEM levels varied from <LOD (2.0 ng m^{-3}) to 48.5 ng m^{-3} (mean 2.7 ng m^{-3}), with no significant differences found among sites. A clear daily pattern emerged, with maximum values reached just after sunset. Air temperature, relative humidity, wind speed and direction were identified as the main micrometeorological factors influencing both the spatial and temporal variation of GEM. Our results show that average atmospheric GEM values are higher than the natural background of the Northern Hemisphere and will be useful in future selection regarding the most suitable sites to monitor atmospheric Hg depositions and fluxes from soil and water.

Keywords: gaseous elemental mercury; Gulf of Trieste; atmospheric Hg transport; sea breeze

1. Introduction

Mercury (Hg) is a well-known global pollutant which is a cause for serious concern regarding ecosystems and human health due to its persistence, toxicity and potential bioaccumulation/biomagnification [1]. The atmosphere represents the main redistribution pathway of Hg mobilised from lithospheric reservoirs and often atmospheric depositions constitute the main source of this element for terrestrial and aquatic ecosystems, even in areas far from points of emission [2]. Once released into the environment, Hg can adversely affect the physiology of many living organisms [3], particularly in its organic form, monomethylmercury (MMHg), which is more toxic and easily biomagnified within the trophic chain due to its lipophilic nature [4]. The consumption of fish contaminated by MMHg is considered the main Hg exposure route for humans [5], whereas inhalation of inorganic Hg vapours occurs mainly via dental amalgams and in certain occupations [6]. Adverse

effects of Hg on human health primarily concern the nervous system, but exposure to the different forms of this element can also damage renal and cardiovascular systems and generate negative reproductive and epigenetic outcomes [7].

As a result of human activities, the amount of Hg mobilised and circulating in the environment showed a sharp increase starting from the preindustrial period. Focusing on the atmospheric compartment, recent estimates show that Hg concentrations increased by approximately 450% above levels which would have been found in the year 1450, which would have been considered pristine conditions [8,9], and also depositions to natural ecosystems have increased by a 3–5 factor compared to preindustrial levels [10]. Anthropogenic Hg emissions into the atmosphere are associated with several activities such as coal combustion, artisanal gold mining, cement and nonferrous metal production, waste incineration, the chlor-alkali industry, etc., and were estimated at 2220 Mg in 2015 [11]. These outputs only account for approximately one-third of the total global Hg released into the atmosphere (6500–8200 Mg year^{-1}), whereas emissions from natural processes range from 4600 to 5300 Mg year^{-1} [12]. However, a large part of these releases are re-emissions of previously deposed Hg from different surfaces (anthropogenic activities oceans, soil, vegetation), while current primary Hg sources such as volcanoes, geothermal activity and weathering of rocks and soils naturally enriched in Hg represent approximately only 4% of total terrestrial outputs [13,14].

Mercury occurs in the atmosphere in three different forms, operationally identified as gaseous elemental Hg (GEM), reactive gaseous Hg (RGM) and particulate bound Hg (PBM) [15]. GEM usually accounts for more than 98% of the total pool [16,17], so its concentrations can be considered indicative of total gaseous Hg levels [18]. This form is very stable in the atmosphere where it can persist for 0.5–2 years [19] and undergo long-range transport before being removed through depositions, thus impacting remote areas such as the Arctic [20]. RGM and PBM, instead, are more soluble (RGM) or easily captured by water (PBM) and show shorter atmospheric lifetimes (hours to days); they are easily removed through wet and dry deposition relatively close to the emission source [21]. Moreover, deposited Hg can be re-emitted back to the atmosphere as GEM, further accentuating the global redistribution of this element [2].

The background value of GEM is currently estimated at 1.5–1.7 ng m^{-3} in the Northern Hemisphere [22], slightly higher than that of the Southern Hemisphere (1.1–1.3 ng m^{-3} [23]) due to the greater abundance of emission and re-emission sources. [24]. However, on the local scale, atmospheric GEM shows notable spatiotemporal variations among different environments owing to the large amount of release and deposition rates [25], which can be influenced by local point-sources, the presence of oxidants in the atmosphere, topography and micrometeorological conditions [26,27]. Moreover, several different diurnal and seasonal patterns of GEM are reported in the literature for marine, coastal, rural and urban environments, making the determination of the predominant controlling factors of observed GEM variation extremely complex ([28] and references therein).

Generally, atmospheric GEM concentrations and variations are often greater in areas subject to strong anthropogenic impact [24]. Spatial and temporal atmospheric GEM trends can be helpful in identifying sources and sinks of Hg in the atmosphere (e.g., [25,29]) and providing useful information for the evaluation of release and dispersion of Hg from sites heavily contaminated by human activities and which should be considered for risk assessment [30,31].

In this work, the levels and spatial distribution of GEM were investigated in the Gulf of Trieste (Northern Adriatic Sea, Italy), a coastal environment historically contaminated by Hg. In this area, the contamination of soil, water and sediments has been well characterised and is the result of secular mining activity which took place in Idrija (NW Slovenia), where high amounts of Hg-contaminated material were dispersed into the environment and then transported by the Isonzo River freshwaters in dissolved and solid forms, flowing into the Gulf [32]. There is, however, still little known about the concentrations, sources and fate of GEM in the atmosphere of this area. To fill the gap, several discrete GEM measurements were conducted at numerous sites characterised by different Hg levels in the substrate, distributed over the coastal areas in order to compare GEM levels from both contaminated

and pristine environments. To better understand temporal patterns and possible dispersion of this contaminant in the atmospheric compartment, continuous night-day measurements were also conducted. Furthermore, GEM values were correlated with the main meteorological parameters in order to elucidate the factors influencing the behaviour of the element in this area.

2. Experiments

2.1. Study Area

The Gulf of Trieste extends from the Tagliamento River mouth to Savudrija/Punta Salvore (Croatia) and covers an area of approximately 550 km^2 in the north easternmost part of the Adriatic Sea. This coastal ecosystem hosts a Marine Protected Area (Miramare) where, due to a no-entry and a buffer zone, conservation and refuge for overexploited species are guaranteed [33]. On the other hand, this densely populated area is host to several varieties of industry. The coastline is largely exploited for tourism (approximately 60%) with Grado and Lignano Sabbiadoro settlements which significantly increase the resident population during summer (from 8000 to 80,000 and 6000 to 250,000, respectively). The most industrialised areas are represented by the cities of Trieste and Monfalcone (210,000 and 30,000 inhabitants, respectively) with their harbours, and also by the nearby city of Koper (Slovenia); overall these industrial sites cover about 30% of the territory (i.e., iron-steel factory, coal-fired power plant, oil pipeline, ship traffic, considerable vehicular emissions and so on). Finally, mussel farming (*Mytilus galloprovincialis*) and aquaculture using suspended cages (*Dicenthrarcus labrax*, *Sparus aurata* and *Mugil cephalus*) take place in the easternmost sector of the Gulf.

Several pollutants (i.e., trace elements and POPs) represent a concern for the area as highlighted in numerous previous studies [34–44]. However, mercury contamination due to secular inland mining exploitation from Idrija (NW Slovenia) shows a wide diffusion in sediments, waters and soils [32,45–47].

2.2. Gaseous Elemental Mercury (GEM) Measurements

GEM measurements were conducted by means of a Lumex RA-915M Portable Mercury Analyzer in selected sites representative of nonurban areas contaminated by Hg (Fossalon-FOS, Grado-GRA and Val Noghera-VN), urban areas (Monfalcone-MON, Villaggio del Pescatore-PES and Trieste-TS) and pristine areas (Basovizza-BAS and Piran-PIR) in the Gulf of Trieste (Northern Adriatic Sea; Figure 1). The Lumex Ra-915M relies on atomic absorption spectrometry (AAS): the instrument has a multipath analytical cell and Zeeman background correction provides both high sensitivity and minimal interference: the accuracy of the method is 20% [48]. The dynamic range covers four orders of magnitude (2–25,000 ng m^{-3}), and the detection limit is governed by shot noise and equals 2.0 ng m^{-3} (average measuring time 5 s) and 0.3 ng m^{-3} (average measuring time 30 s). A complete calibration is done by a Lumex technician each year, while a calibration check of the instrument is performed prior to taking measurements by means of an internal accessory cell containing a known amount of Hg. During field work, real-time measurements were visualised on a digital display and stored in an internal data logger. Subsequently, the data were recovered by RAPID 1.00.442 software.

The data were acquired over a variable time range, from a few hours to a maximum of 14 days, depending on sites and local conditions, and sampling rate (from 1 to 10 s). Moreover, values below 2 ng m^{-3} were treated with the medium bound approach, thus set to $\frac{1}{2}$ LOD (1 ng m^{-3}). All GEM time-series were resampled to a fixed sampling frequency of 1 h in order to easily process the dataset and check the relationships with some meteorological parameters provided by the "OMNIA" database from the meteorological observatory of the regional environmental protection agency (OSMER–ARPA FVG, Visco, Italy).

Univariate statistics were computed hourly with Microsoft Excel spreadsheets and then processed in Python. The Pandas library [49] was employed for time-series downsampling and re-sampling and for calculating matrices of Spearman nonparametric correlation coefficient. The wind rose chart

(or polar bar chart) was obtained using the Plotly library [50] graphic tool. All time data are expressed in UTC+0 (Greenwich Mean Time; GMT).

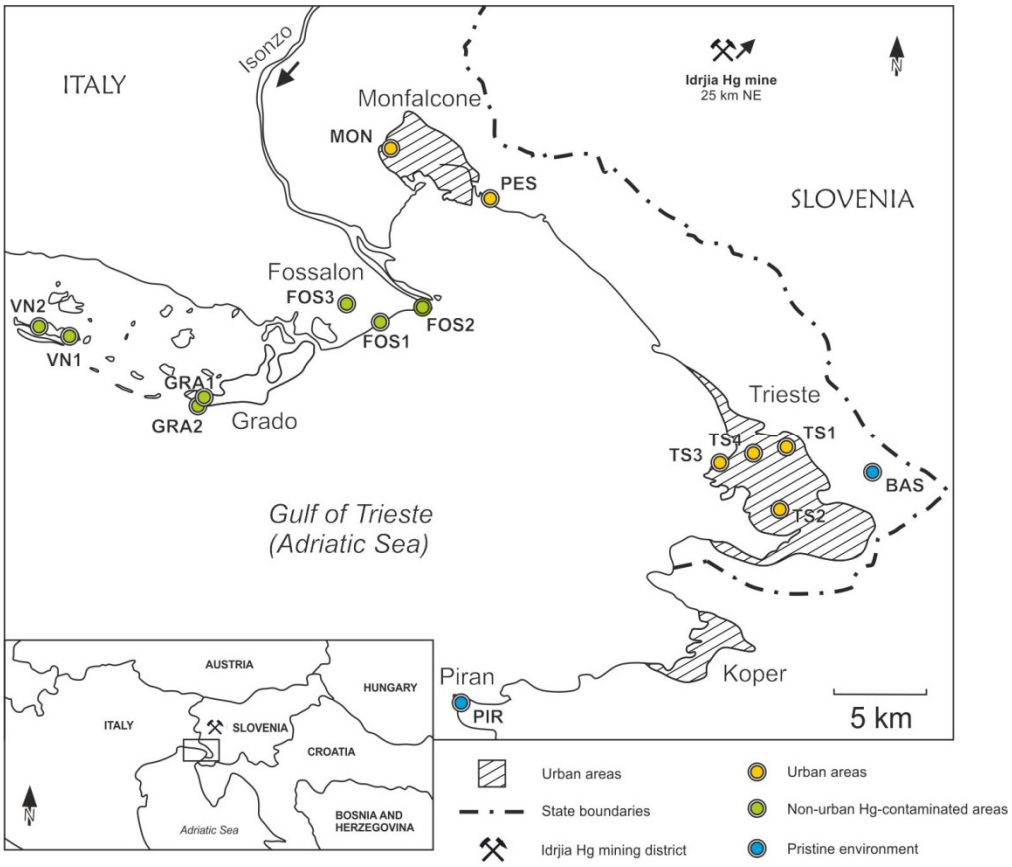

Figure 1. Study area and selected sampling sites: on the lower left the symbol shows the location of the Idrija Hg mine responsible for the contamination of the Isonzo River Plain and the Gulf of Trieste.

3. Results and Discussion

3.1. GEM Level and Distribution

The univariate descriptive statistic of the surveyed sites is reported in Table 1. As previously mentioned, the pristine environment was chosen for its suitability for comparison with other impacted sites at a considerable distance from Hg-bearing sediments and soils affected by the mining activity of the Idrija Hg mine and from other potential emissions. These sites (BAS and PIR) were previously investigated and showed GEM contents that were on average lower than those found in the other sites (1.02 ± 0.32 and 1.88 ± 1.07 ng m^{-3}, respectively) [51,52]. It is notable that MON, which is located in an urban area, showed lower values (1.19 ± 0.40 ng m^{-3}) considering the hourly average, but the maximum reached up to 17.28 ng m^{-3}. Overall, mean hourly values ranged between 1.20 and 3.57 ng m^{-3}, comparable or slightly higher than the natural background levels estimated for the Northern Hemisphere (1.5–1.7 ng m^{-3}) [22] and for the Mediterranean area (1.75–1.80 ng m^{-3}) [53]. The highest concentrations were found at the Hg-contaminated FOS site (48.5 ng m^{-3}). This area was originally part of the Isonzo River delta and has been affected by human activity since 1800, in particular by land reclamation (several dewatering plants) for intensive agriculture which took place after 1920: the soils are heavily contaminated (up to 40 mg kg^{-1}) [54].

Table 1. Basic statistics of gaseous elemental mercury (GEM) dataset calculated on raw data (not resampled) and grouped by location. (*) Data published by [52] and (§) [51].

	SITE	GEM Mean (ng m^{-3})	GEM dev. st. (ng m^{-3})	GEM Max (ng m^{-3})	N Data	Lat. (WGS84)	Lon. (WGS84)	Altitude (m m.s.l.)
Non-urban Hg-contaminated areas	FOSSALON	3.57	1.44	48.46	914,493			
	FOS1	4.14	1.48	18.18	374,127	45.718837	13.516823	0
	FOS2	2.83	1.45	48.46	161,700	45.728359	13.536141	0
	FOS3	3.30	1.40	47.63	378,666	45.719781	13.492587	0
	GRADO	2.74	0.85	13.99	278,026			
	GRA1	1.85	0.76	8.48	47,599	45.682133	13.390340	0
	GRA2	3.48	0.94	13.99	230,427	45.678219	13.388133	1
	VAL NOGHERA [*]	2.12	1.16	9.52	17,372			
	VN1	2.28	1.27	9.52	8204	45.710263	13.308906	0
	VN2	1.98	1.06	8.03	9168	45.713665	13.288101	0
Urban areas	MONFALCONE	1.19	0.40	17.28	22,910			
	MON	1.19	0.40	17.28	22,910	45.801200	13.528419	5
	VILLAGGIO DEL PESCATORE	2.53	0.94	8.61	219,138			
	PES	2.53	0.94	8.61	219,138	45.777859	13.588559	0
	TRIESTE	2.56	1.20	26.46	1,845,127			
	TS1	2.36	1.14	21.24	1,681,994	45.658275	13.800820	80
	TS2	3.26	1.62	26.46	84,186	45.623776	13.803742	40
	TS3	4.43	1.12	13.77	28,540	45.647045	13.764987	10
	TS4	3.07	1.43	10.02	50,407	45.656577	13.784282	30
Pristine areas	BASOVIZZA [§]	1.20	0.32	2.80	2676			
	BAS	1.20	0.32	2.80	2676	45.641365	13.862287	380
	PIRAN [*]	1.88	1.07	8.60	7506			
	PIR	1.88	1.07	8.60	7506	45.518672	13.568036	0

These results are comparable to those found in other Hg-contaminated sites. Taking as an example, Muramoto et al. [55] recorded GEM ranging from 1.89 to 2.23 ng m^{-3} (max = 6.11 ng m^{-3}) in the Minamata Bay (Japan). In the Mediterranean area Bagnato et al. 2013 [56] and Gibicar et al. 2009 [57] found from 1.5 ± 0.4 to 2.1 ± 0.98 and from 2.8 to 8.7 ng m^{-3} in the Augusta Bay (Sicily, Italy) and Rosignano (Tuscany, Italy), respectively, and the GEM values were higher during the summer period.

Due to the large amount of the dataset, the comparison of GEM concentrations was depicted by means of a box and whisker plot representation. Briefly, the median is represented by the horizontal bold line within the box, 25th and 75th percentiles are at the top and bottom. In this case, the presence of outliers is shown as circles if values are 1.5 times out of the box and as stars for values which are three times out of the box (Figure 2). Site FOS showed several outliers such as TS, thus suggesting that there are nearby sources of GEM (i.e., contaminated soils, urban activities) that, in the absence of dilution conditions, can be detected by means of continuous monitoring. On the other hand, pristine areas do not behave like active GEM sources and show data comparable to those observed in other areas (ranging from 0.3 to 10 ng m^{-3}) with no outliers [31]. The significant difference between sample medians was confirmed by the Kruskal–Wallis test (p = same = 2.18×10^{-71}), which is a nonparametric method for testing if there are statistically significant differences between two or more groups of an independent variable. The calculated ratio of urban to pristine site concentrations for GEM, on average, usually range from 1 to 1.8 [27], and the ratio found in this study, which is 1.52, falls within the ranges from other pristine-urban site studies.

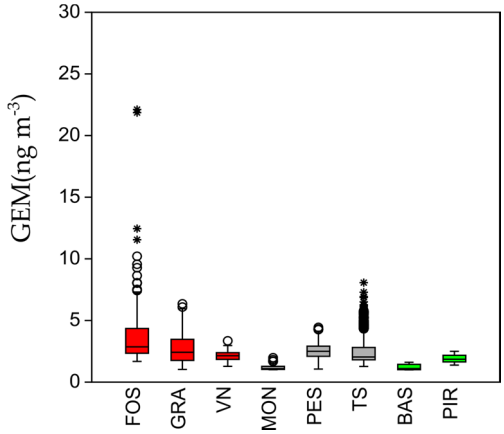

Figure 2. Boxplots of GEM observed in the investigated sites. (**red**) Hg-contaminated sites; (**grey**) urban sites; (**green**) nonurban and pristine sites.

One of the main concerns arising from GEM levels is the potential risk for local inhabitants via an inhalation pathway. According to the guidelines and safety regulations reported in Oyarzun et al. [58], it can be asserted that no risk is present for local inhabitants (WHO guideline fixed at 1000 ng m^{-3}; MRL for chronic inhalation 200 ng m^{-3}, US OSHA and ATSDR).

3.2. GEM Time-Series

One of the goals of this study was to investigate the occurrence of daily cycles of GEM concentrations as previously reported for other contaminated sites [31]. In this context, some particular time-series, the monitoring campaigns in Fossalon (FOS3_1 and FOS1_2, 2013 and 2015), Grado (GRA2_1, 2015) and Trieste (TS2_3, 2015), are reported in Figure 3.

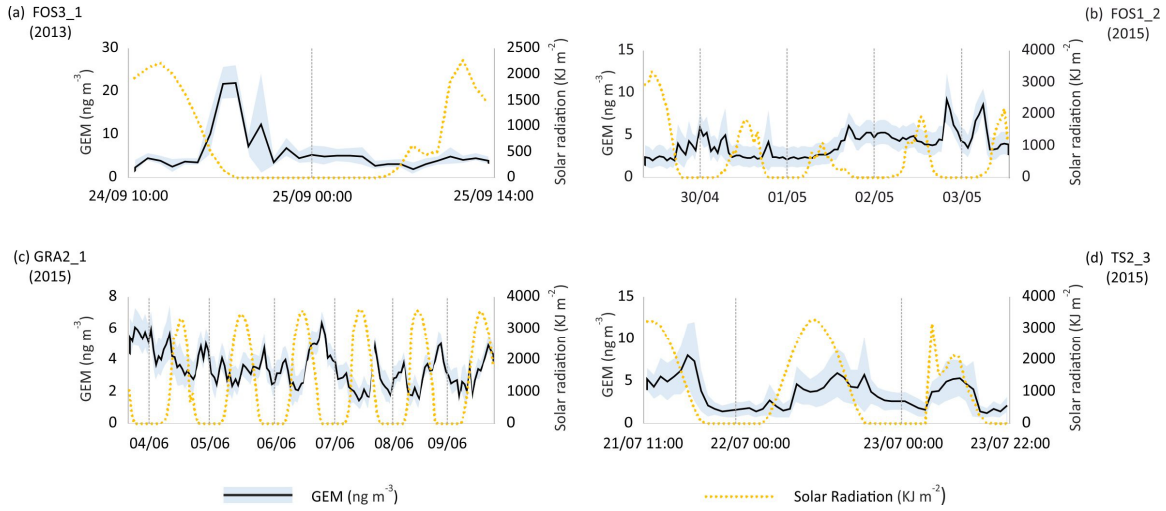

Figure 3. Time-series of GEM (ng m^{-3}) plotted against intensity of solar radiation (kJ m^{-2}) at selected sites. Date is expressed as dd/mm. (**a**,**b**) Fossalon Hg-contaminated site; (**c**) Grado Hg-contaminated site; (**d**) Trieste urban area.

The time-series at FOS3_1 showed the presence of anomalous brief high-amplitude peaks that occurred at sunset and during the night (Figure 3a). As previously mentioned, values up to 48.46 ng m^{-3} were reached (Table 1). In other cases, the peaks were less high in amplitude but more frequent (Figure 3b,c). It can be hypothesised that the contaminated soils are characterised by an emission capacity, a continuous source of GEM that is generally higher during the day because of incident solar radiation. However, during sunrise the temperature decreases and the sea breeze drops;

before the opposite land breeze occurs, a temporary atmospheric stable condition is created so that atmospheric dilution and mixing are not favoured, and GEM can concentrate in the lower layers of the atmosphere [30,31].

The occurrence of events of high atmospheric GEM levels is usually associated with conditions of stagnant air and low atmospheric mixing as shown in Figure 4 [17,59].

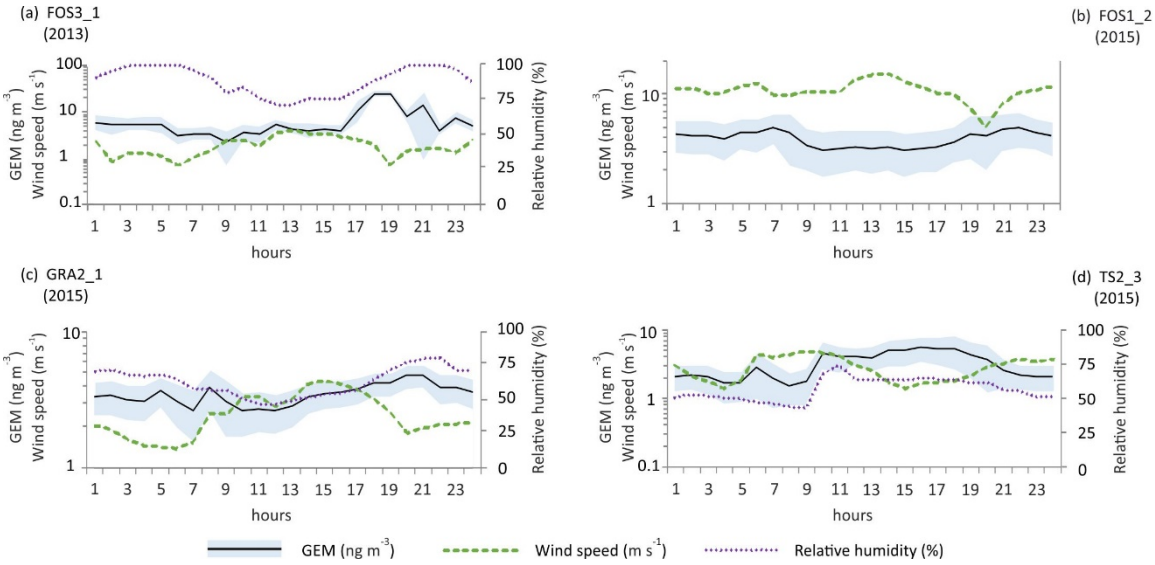

Figure 4. Hourly average values of GEM (ng m^{-3}) plotted against wind speed (m s^{-1}) and relative humidity at selected sites. (**a**,**b**) Fossalon Hg-contaminated site; (**c**) Grado Hg-contaminated site; (**d**) Trieste urban area.

During diurnal hours, sea breezes can dilute atmospheric GEM, resulting in lower concentrations. However, considering that the correlation between wind speed and GEM (Table 2) is below 0.3, we hypothesise that lower levels of this contaminant during the day at the Fossalon site could also be caused by an enhanced photooxidation to RGM, which can easily be removed from the atmosphere through atmospheric depositions [60]. In coastal areas, air coming from the sea driven by breezes is usually rich in oxidants such as halogen radicals (e.g., bromine), which are thought to favour the oxidation of GEM in the presence of solar radiation [61,62] and in the marine boundary layer the reaction of GEM with bromine is considered the predominant pathway of oxidation for this species [63].

Table 2. Spearman (r) correlation matrix between GEM concentrations and micrometeorological parameters. Dark blue and red indicate strong negative and positive significant correlations.

	Site	Temperature	Solar Radiation	Wind Speed	Wind Direction	Relative Humidity	Season
Non-urban Hg-contaminated sites	FOS1_2	−0.25	−0.42	−0.30	−0.17		Spring
	FOS2_1	0.02	−0.14	−0.26	0.09	0.07	Spring
	FOS3_1	−0.36	−0.44	−0.16	−0.19	0.38	Autumn
	GRA2_1	−0.31	−0.26	0.25	0.08	0.72	Summer
	GRA1_1	−0.12	−0.54	−0.20	−0.32	0.22	Autumn
	PES_1	0.47	0.43	0.18	0.24	−0.18	Summer
Urban sites	TS1_4	0.26	−0.02	−0.27	0.18	0.49	Spring
	TS3_1	0.11	0.53	0.34	0.17	−0.11	Spring
	TS1_5	−0.05	−0.02	−0.02	−0.07	−0.08	Summer
	TS2_3	0.16	0.63	−0.49	0.60	0.79	Summer
	TS1_6	0.22	−0.16	−0.48	0.21	0.51	Autumn

On the contrary, the GEM content in the urban area of Trieste appears to be influenced by solar radiation (Figure 3d).

To assess the correlation between GEM and micrometeorological parameters, Spearman's correlation coefficients were calculated for any time-series longer than 24 h (Table 2). Generally, we found that GEM reached its highest values when air relative humidity raised, likely because they have similar behaviour with respect to wind dilution. High relative air humidity is usually associated with stagnant atmospheric conditions, which as stated above favours the accumulation of GEM in the lower atmosphere. Taking as an example the measurements conducted at Grado, a significant correlation of GEM with air relative humidity (r = 0.72; Table 2) occurred at GRA2_1 during six days of continuous monitoring. Moreover, GEM increases with temperature, and the behaviour of GEM differs between the Hg-contaminated soil of the Isonzo River Plain and lagoon, and the city of Trieste. In the first case, GEM showed negative correlations with solar radiation, whereas it showed the opposite trend in the urban area of Trieste. This difference is likely a consequence of the distribution of breeze strength between the considered sites; the Isonzo alluvial plain is characterised by a diurnal sea breeze stronger than a nocturnal land breeze, whereas the urban area of Trieste shows an opposite pattern, with higher speeds during the night. In this urban site, no relevant sources of contamination are known, thus GEM could largely be carried from contaminated areas by wind during the diurnal sea breeze. The influence of sea breezes on atmospheric GEM levels in urban areas is well documented [17,25,61,64].

The wind rose chart shows that when GEM is high (up to an hourly mean value of 8 ng m^{-3}) with winds prevalently blowing from W and NW, in the direction of the highly contaminated Fossalon plain, it (GEM) could reach the city of Trieste via the seawater surface of the Gulf (Figure 5). It was hypothesised that a variation in wind speed is not sufficient to cause a dilution process responsible for the decrease in GEM during the night. A possible explanation could instead be that there is another significant source of GEM in the area. This could be represented by the waters of the Gulf of Trieste itself, since it is well-known that elemental Hg can be transferred not only between mining-impacted marine sediments and seawater, but also from seawater to the surrounding inhabited coastal area. In a previous study, Wänberg et al. [53] found that atmospheric GEM levels in Piran follow a similar pattern, showing higher values under conditions of low wind speed blowing from the north. The authors postulated that these air masses were enriched in GEM while passing over the contaminated gulf due to GEM emission from the surface of the sea, a process potentially relevant thanks to the abundance in the water column of this area of dissolved Hg available for reduction and subsequent volatilisation [46,65]. Unfortunately, no data regarding GEM in the Gulf of Trieste are available to more strongly support this hypothesis.

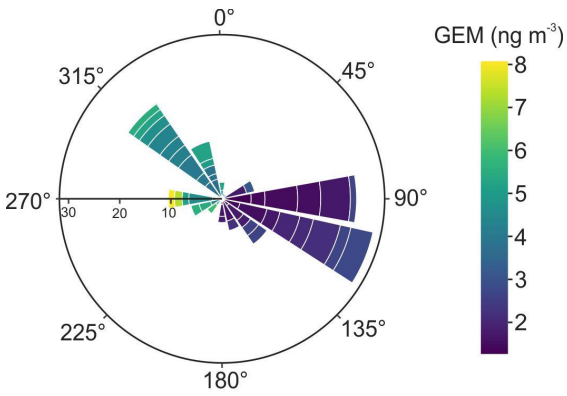

Figure 5. Wind rose for GEM data at Trieste (time-series: TS2_3). Colours indicate GEM concentration, while the radius length is the cumulative wind speed (m s^{-1}).

4. Conclusions

This study provides new data regarding gaseous elemental mercury (GEM) in the atmosphere around the Gulf of Trieste, which is a historically Hg-contaminated coastal area via sediment/soil-associated metal dispersion from the Isonzo River resulting from mercury mining from Idrija. The results of the study show that GEM concentrations do not reach levels of concern for the population. However, significant variations of GEM have been observed, showing that the coastal alluvial plain built up along the Isonzo River is an active source of mercury in the atmosphere. Anomalous peaks of GEM have been observed, especially at sunset or during the night, when the sea breeze turns into the land breeze, resulting in a decrease in wind speed and scarce low mixing of the low atmospheric layer in contact with the ground. These sites with high-amplitude plumes of GEM are also worth long-term monitoring for continuous data acquisition.

In the urban area of Trieste, the correlation between wind direction and GEM indicates a mass flow of GEM transported from the Isonzo coastal alluvial plain without excluding a contribution from coastal waters of the Gulf to the surrounding areas. The main difference between the nonurban contaminated land/lagoon and the urban area investigated is a different day-night pattern of GEM distribution. On the sites contaminated by Hg, GEM tends to be higher during the night, whereas urban areas show an opposite trend, with maximum values reached during the day. A possible explanation is that in the urban area, anthropogenic Hg emissions contributed significantly to the atmospheric GEM budget, whereas releases from contaminated soils at Fossalon are mainly driven by natural re-emission processes. Further research is needed to identify and quantify the emission sources in both environments, also including monitoring of other trace gases (e.g., CO_2, CO, CH_4, SO_2) usually used as signatures of anthropogenic influence. Future study is also required to understand the contribution of atmospheric Hg deposition to the observed daily GEM patterns, to determine whether their contribution to GEM depletion is higher than that of atmospheric mixing and transport, particularly at those sites which showed a higher daily variability (e.g., over the Isonzo coastal alluvial plain). Moreover, determination of the different atmospheric Hg species, together with measurements of atmospheric oxidants such as halogen radicals, could give further information regarding GEM oxidation to RGM, which could be particularly relevant for coastal environments and contribute to the enhancement of Hg deposition on the substrate.

Author Contributions: Data curation, conceptualization, methodology, writing-original draft and writing review N.B., F.F., S.C., J.M.E., P.H. and A.A. Processing of data N.B. Data survey N.B., F.F., P.H. and S.C. Final editing A.A. All authors have read and agreed to the published version of the manuscript.

Funding: This research received no external funding.

Acknowledgments: Two anonymous reviewers are warmly acknowledged for their reviews and useful suggestions which improved the earlier version of the manuscript. Karry Close is warmly acknowledged for proofreading the manuscript.

Conflicts of Interest: The authors declare no conflict of interest.

References

1. Beckers, F.; Rinklebe, J. Cycling of mercury in the environment: Sources, fate, and human health implications: A review. *Crit. Rev. Environ. Sci. Technol.* **2017**, *47*, 693–794. [CrossRef]
2. Selin, N.E. Global biogeochemical cycling of mercury: A review. *Annu. Rev. Environ. Resour.* **2009**, *34*, 43–63. [CrossRef]
3. Boening, D.W. Ecological effects, transport, and fate of mercury: A general review. *Chemosphere* **2000**, *40*, 1335–1351. [CrossRef]
4. Morel, F.M.M.; Kraepiel, A.M.L.; Amyot, M. The chemical cycle and bioaccumulation of mercury. *Annu. Rev. Ecol. Syst.* **1998**, *29*, 543–566. [CrossRef]
5. Fitzgerald, W.F.; Clarkson, T.W. Mercury and monomethylmercury: Present and future concerns. *Environ. Health Perspect.* **1991**, *96*, 159–166. [CrossRef] [PubMed]

6. Rice, K.M.; Walker, E.M.; Wu, M.; Gillette, C.; Blough, E.R. Environmental mercury and its toxic effects. *J. Prev. Med. Public Health* **2014**, *47*, 74–83. [CrossRef] [PubMed]
7. Kim, K.H.; Kabir, E.; Jahan, S.A. A review on the distribution of Hg in the environment and its human health impacts. *J. Hazard. Mater.* **2016**, *306*, 376–385. [CrossRef]
8. Zhang, Y.; Jaeglé, L.; Thompson, L.; Streets, D.G. Six centuries of changing oceanic mercury. *Glob. Biogeochem. Cycles* **2014**, 1251–1261. [CrossRef]
9. Outridge, P.M.; Mason, R.P.; Wang, F.; Guerrero, S.; Heimbürger-Boavida, L.E. Updated global and oceanic mercury budgets for the United Nations global mercury assessment 2018. *Environ. Sci. Technol.* **2018**, *52*, 11466–11477. [CrossRef]
10. Mason, R.P.; Sheu, G.R. Role of the ocean in the global Mercury CYCLE. *Glob. Biogeochem. Cycles* **2002**, *16*, 40–41. [CrossRef]
11. UN Environment. *Global Mercury Assessment 2018*; UN Environment Programme: Geneva, Switzerland, 2019.
12. Driscoll, C.T.; Mason, R.P.; Chan, H.M.; Jacob, D.J.; Pirrone, N. Mercury as a global pollutant: Sources, pathways, and effects. *Environ. Sci. Technol.* **2013**, *47*, 4967–4983. [CrossRef] [PubMed]
13. Pirrone, N.; Cinnirella, S.; Feng, X.; Finkelman, R.B.; Friedli, H.R.; Leaner, J.; Mason, R.; Mukherjee, A.B.; Stracher, G.B.; Streets, D.G.; et al. Global mercury emissions to the atmosphere from anthropogenic and natural sources. *Atmos. Chem. Phys.* **2010**, *10*, 5951–5964. [CrossRef]
14. Sundseth, K.; Pacyna, J.M.; Pacyna, E.G.; Pirrone, N.; Thorne, R.J. Global sources and pathways of mercury in the context of human health. *Int. J. Environ. Res. Public Health* **2017**, *14*. [CrossRef] [PubMed]
15. Poissant, L.; Pilote, M.; Beauvais, C.; Constant, P.; Zhang, H.H. A year of continuous measurements of three atmospheric mercury species (GEM, RGM and Hgp) in Southern Québec, Canada. *Atmos. Environ.* **2005**, *39*, 1275–1287. [CrossRef]
16. Slemr, F.; Schuster, G.; Seiler, W. Distribution, speciation, and budget of atmospheric mercury. *J. Atmos. Chem.* **1985**, *3*, 407–434. [CrossRef]
17. Griggs, T.; Liu, L.; Talbot, R.W.; Torres, A.; Lan, X. Comparison of atmospheric mercury speciation at a coastal and an urban site in southeastern Texas, USA. *Atmosphere* **2020**, *11*. [CrossRef]
18. Mao, H.; Talbot, R.W.; Sigler, J.M.; Sive, B.C.; Hegarty, J.D. Seasonal and diurnal variations of Hg&Deg; over New England. *Atmos. Chem. Phys.* **2008**, *8*, 1403–1421. [CrossRef]
19. Schroeder, W.H.; Munthe, J. Atmospheric mercury—An overview. *Atmos. Environ.* **1998**, *32*, 809–822. [CrossRef]
20. Travnikov, O. Contribution of the intercontinental atmospheric transport to mercury pollution in the northern hemisphere. *Atmos. Environ.* **2005**, *39*, 7541–7548. [CrossRef]
21. Valente, R.J.; Shea, C.; Lynn Humes, K.; Tanner, R.L. Atmospheric mercury in the great smoky mountains compared to regional and global levels. *Atmos. Environ.* **2007**, *41*, 1861–1873. [CrossRef]
22. Sprovieri, F.; Pirrone, N.; Ebinghaus, R.; Kock, H.; Dommergue, A. A review of worldwide atmospheric mercury measurements. *Atmos. Chem. Phys.* **2010**, *10*, 8245–8265. [CrossRef]
23. Lindberg, S.; Bullock, R.; Ebinghaus, R.; Engstrom, D.; Feng, X.; Fitzgerald, W.; Pirrone, N.; Prestbo, E.; Seigneur, C. A synthesis of progress and uncertainties in attributing the sources of mercury in deposition. *Ambio* **2007**, *36*, 19–32. [CrossRef]
24. Sprovieri, F.; Pirrone, N.; Bencardino, M.; D'Amore, F.; Carbone, F.; Cinnirella, S.; Mannarino, V.; Landis, M.; Ebinghaus, R.; Weigelt, A.; et al. Atmospheric mercury concentrations observed at ground-based monitoring sites globally distributed in the framework of the GMOS network. *Atmos. Chem. Phys.* **2016**, *16*, 11915–11935. [CrossRef] [PubMed]
25. Lan, X.; Talbot, R.; Laine, P.; Lefer, B.; Flynn, J.; Torres, A. Seasonal and diurnal variations of total gaseous mercury in urban Houston, TX, USA. *Atmosphere* **2014**, *5*, 399–419. [CrossRef]
26. Rutter, A.P.; Snyder, D.C.; Stone, E.A.; Schauer, J.J.; Gonzalez-Abraham, R.; Molina, L.T.; Ḿarquez, C.; Ćardenas, B.; De Foy, B. In situ measurements of speciated atmospheric mercury and the identification of source regions in the Mexico City metropolitan area. *Atmos. Chem. Phys.* **2009**, *9*, 207–220. [CrossRef]
27. Cheng, I.; Zhang, L.; Mao, H.; Blanchard, P.; Tordon, R.; Dalziel, J. Seasonal and diurnal patterns of speciated atmospheric mercury at a coastal-rural and a coastal-urban site. *Atmos. Environ.* **2014**, *82*, 193–205. [CrossRef]
28. Mao, H.; Cheng, I.; Zhang, L. Current understanding of the driving mechanisms for spatiotemporal variations of atmospheric speciated mercury: A review. *Atmos. Chem. Phys.* **2016**, *16*, 12897–12924. [CrossRef]

29. Ren, X.; Luke, W.T.; Kelley, P.; Cohen, M.D.; Artz, R.; Olson, M.L.; Schmeltz, D.; Puchalski, M.; Goldberg, D.L.; Ring, A.; et al. Atmospheric mercury measurements at a suburban site in the mid-atlantic united states: Inter-annual, seasonal and diurnal variations and source-receptor relationships. *Atmos. Environ.* **2016**, *146*, 141–152. [CrossRef]
30. Esbrí, J.M.; Martínez-Coronado, A.; Higueras, P.L. Temporal variations in gaseous elemental mercury concentrations at a contaminated Site: Main factors affecting nocturnal maxima in daily cycles. *Atmos. Environ.* **2016**, *125*, 8–14. [CrossRef]
31. Higueras, P.; Oyarzun, R.; Kotnik, J.; Esbrí, J.M.; Martínez-Coronado, A.; Horvat, M.; López-Berdonces, M.A.; Llanos, W.; Vaselli, O.; Nisi, B.; et al. A compilation of field surveys on gaseous elemental mercury (GEM) from contrasting environmental settings in Europe, South America, South Africa and China: Separating fads from facts. *Environ. Geochem. Health* **2014**, *36*, 713–734. [CrossRef]
32. Covelli, S.; Faganeli, J.; Horvat, M.; Brambati, A. Mercury contamination of coastal sediments as the result of long-term cinnabar mining activity (gulf of Trieste, Northern Adriatic Sea). *Appl. Geochem.* **2001**, *16*, 541–558. [CrossRef]
33. Boero, F.; Brian, F.; Micheli, F. Scientific design and monitoring of mediterranean marine protected areas. In Proceedings of the CIESM Workshop Series No 8, Porto Cesareo, Italy, 21–24 October 1999; p. 64.
34. Olivotti, R.; Faganeli, J.; Malej, A. Impact of "organic" pollutants on coastal waters, gulf of Trieste. *Water Sci. Technol.* **1986**, *18*, 57–68. [CrossRef]
35. Adami, G.; Barbieri, P.; Piselli, S.; Predonzani, S.; Reisenhofer, E. New data on organic pollutants in surface sediments in the harbour of Trieste. *Ann. Chim.* **1998**, *88*, 745–754.
36. Pozo, K.; Lazzerini, D.; Perra, G.; Volpi, V.; Corsolini, S.; Focardi, S. Levels and spatial distribution of polychlorinated biphenyls (PCBs) in superficial sediment from 15 Italian Marine Protected Areas (MPA). *Mar. Pollut. Bull.* **2009**, *58*, 773–776. [CrossRef] [PubMed]
37. Adami, G.; Barbieri, P.; Piselli, S.; Predonzani, S.; Reisenhofer, E. Detecting and characterising sources of persistent organic pollutants (PAHs and PCBs) in surface sediments of an industrialized area (harbour of Trieste, Northern Adriatic Sea). *J. Environ. Monit.* **2000**, *2*, 261–265. [CrossRef]
38. Formalewicz, M.; Rampazzo, F.; Noventa, S.; Gion, C.; Petranich, E.; Crosera, M.; Covelli, S.; Faganeli, J.; Berto, D. Organotin compounds in touristic marinas of the Northern Adriatic sea: Occurrence, speciation and potential recycling at the sediment-water interface. *Environ. Sci. Pollut. Res.* **2019**, *26*, 31142–31157. [CrossRef] [PubMed]
39. Barbieri, P.; Adami, G.; Predonzani, S.; Reisenhofer, E. Heavy metals in surface sediments near urban and industrial sewage discharges in the gulf of Trieste. *Toxicol. Environ. Chem.* **1999**, *71*, 105–114. [CrossRef]
40. Cibic, T.; Acquavita, A.; Aleffi, F.; Bettoso, N.; Blasutto, O.; De Vittor, C.; Falconi, C.; Falomo, J.; Faresi, L.; Predonzani, S.; et al. Integrated approach to sediment pollution: A case study in the gulf of Trieste. *Mar. Pollut. Bull.* **2008**, *56*, 1650–1657. [CrossRef]
41. Milivojevič Nemanič, T.; Leskovšek, H.; Horvat, M.; Vrišer, B.; Bolje, A. Organotin compounds in the marine environment of the bay of Piran, Northern Adriatic sea. *J. Environ. Monit.* **2002**, *4*, 426–430. [CrossRef]
42. Ščančar, J.; Zuliani, T.; Turk, T.; Milačič, R. Organotin compounds and selected metals in the marine environment of Northern Adriatic sea. *Environ. Monit. Assess.* **2007**, *127*, 271–282. [CrossRef]
43. Acquavita, A.; Predonzani, S.; Mattassi, G.; Rossin, P.; Tamberlich, F.; Falomo, J.; Valic, I. Heavy metal contents and distribution in coastal sediments of the gulf of Trieste (NORTHERN Adriatic sea, Italy). *Water. Air. Soil Pollut.* **2010**, *211*, 95–111. [CrossRef]
44. Petranich, E.; Croce, S.; Crosera, M.; Pavoni, E.; Faganeli, J.; Adami, G.; Covelli, S. Mobility of Metal(Loid)s at the Sediment-Water Interface in Two Tourist Port Areas of the Gulf of Trieste (Northern Adriatic sea). *Environ. Sci. Pollut. Res.* **2018**, *25*, 26887–26902. [CrossRef] [PubMed]
45. Horvat, M.; Covelli, S.; Faganeli, J.; Logar, M.; Mandić, V.; Rajar, R.; Širca, A.; Žagar, D. Mercury in contaminated coastal environments. A case study: The gulf of Trieste. *Sci. Total Environ.* **1999**, *237–238*, 43–56. [CrossRef]
46. Faganeli, J.; Horvat, M.; Covelli, S.; Fajon, V.; Logar, M.; Lipej, L.; Cermelj, B. Mercury and methylmercury in the gulf of Trieste (Northern Adriatic sea). *Sci. Total Environ.* **2003**, *304*, 315–326. [CrossRef]
47. Piani, A.; Acquavita, A.; Catalano, L.; Contin, M.; Mattassi, G.; De Nobili, M. Effects of long term Hg contamination on soil mercury speciation and soil biological activities. *E3S Web Conf.* **2013**, *1*, 1–4. [CrossRef]

48. Sholupov, S.E.; Ganeyev, A.A. Zeeman atomic absorption spectrometry using high frequency modulated light polarization. *Spectrochim. Acta Part B At. Spectrosc.* **1995**, *50*, 1227–1236. [CrossRef]
49. McKinney, W. Data structures for statistical computing in Python. In Proceedings of the 9th Python in Science Conference, Austin, TX, USA, 28 June–3 July 2010; Volume 1697900, pp. 51–56.
50. Sievert, C.; Parmer, C.; Hocking, T.; Chamberlain, S.; Ram, K.; Corvellec, M.; Despouy, P. Plotly: Create Interactive Web Graphics via "Plotly. Js.". 2018. Available online: https://rdrr.io/cran/plotly/ (accessed on 28 August 2020).
51. Acquavita, A.; Biasiol, S.; Lizzi, D.; Mattassi, G.; Pasquon, M.; Skert, N.; Marchiol, L. Gaseous elemental mercury level and distribution in a heavily contaminated site: The ex-chlor alkali plant in torviscosa (Northern Italy). *Water. Air. Soil Pollut.* **2017**, *228*. [CrossRef]
52. Floreani, F.; Acquavita, A.; Petranich, E.; Covelli, S. Diurnal fluxes of Gaseous elemental mercury from the water-air interface in coastal environments of the Northern Adriatic sea. *Sci. Total Environ.* **2019**, *668*, 925–935. [CrossRef]
53. Wängberg, I.; Munthe, J.; Amouroux, D.; Andersson, M.E.; Fajon, V.; Ferrara, R.; Gårdfeldt, K.; Horvat, M.; Mamane, Y.; Melamed, E.; et al. Atmospheric mercury at Mediterranean coastal stations. *Environ. Fluid Mech.* **2008**, *8*, 101–116. [CrossRef]
54. Acquavita, A.; Brandolin, D.; Felluga, A.; Maddaleni, P.; Meloni, C.; Poli, L.; Skert, N.; Zanello, A. Mercury distribution and speciation in soils contaminated by historically mining activity: The Isonzo River plain. In Proceedings of the Congresso SIMP-SGI-SOGEI 2019, Parma, Italy, 16–19 September 2019.
55. Marumoto, K.; Hayashi, M.; Takami, A. Atmospheric mercury concentrations at two sites in the Kyushu Islands, Japan, and evidence of long-range transport from East Asia. *Atmos. Environ.* **2015**, *117*, 147–155. [CrossRef]
56. Bagnato, E.; Sproveri, M.; Barra, M.; Bitetto, M.; Bonsignore, M.; Calabrese, S.; Di Stefano, V.; Oliveri, E.; Parello, F.; Mazzola, S. The sea-air exchange of mercury (Hg) in the marine boundary layer of the Augusta Basin (Southern Italy): Concentrations and evasion flux. *Chemosphere* **2013**, *93*, 2024–2032. [CrossRef] [PubMed]
57. Gibičar, D.; Horvat, M.; Logar, M.; Fajon, V.; Falnoga, I.; Ferrara, R.; Lanzillotta, E.; Ceccarini, C.; Mazzolai, B.; Denby, B.; et al. Human exposure to mercury in the vicinity of chlor-alkali plant. *Environ. Res.* **2009**, *109*, 355–367. [CrossRef] [PubMed]
58. Oyarzun, R.; Higueras, P.; Esbrí, J.M.; Pizarro, J. Mercury in air and plant specimens in herbaria: A pilot study at the MAF herbarium in Madrid (Spain). *Sci. Total Environ.* **2007**, *387*, 346–352. [CrossRef]
59. Nie, X.; Mao, H.; Li, P.; Li, T.; Zhou, J.; Wu, Y.; Yang, M.; Zhen, J.; Wang, X.; Wang, Y. Total gaseous mercury in a coastal city (Qingdao, China): Influence of sea-land breeze and regional transport. *Atmos. Environ.* **2020**, *235*, 1–11. [CrossRef]
60. Amos, H.M.; Jacob, D.J.; Holmes, C.D.; Fisher, J.A.; Wang, Q.; Yantosca, R.M.; Corbitt, E.S.; Galarneau, E.; Rutter, A.P.; Gustin, M.S.; et al. Gas-particle partitioning of atmospheric Hg (II) and its effect on global mercury deposition. *Atmos. Chem. Phys.* **2012**, *12*, 591–603. [CrossRef]
61. Malcolm, E.G.; Keeler, G.J.; Landis, M.S. The effects of the coastal environment on the atmospheric mercury cycle. *J. Geophys. Res.* **2003**, *108*, 1–10. [CrossRef]
62. Lyman, S.N.; Cheng, I.; Gratz, L.E.; Weiss-Penzias, P.; Zhang, L. An updated review of atmospheric mercury. *Sci. Total Environ.* **2020**, *707*, 55–75. [CrossRef]
63. Holmes, C.D.; Jacob, D.J.; Mason, R.P.; Jaffe, D.A. Sources and deposition of reactive gaseous mercury in the marine atmosphere. *Atmos. Environ.* **2009**, *43*, 2278–2285. [CrossRef]
64. Bełdowska, M.; Falkowska, L.; Siudek, P.; Gajecka, A.; Lewandowska, A.; Rybka, A.; Zgrundo, A. Atmospheric mercury over the coastal zone of the gulf of Gda ń Sk oceanological and hydrobiological studies atmospheric mercury over the coastal zone of the gulf of Gda ń Sk. *Int. J. Oceanogr. Hydrobiol.* **2007**, *36*, 1–10.
65. Bratkič, A.; Tinta, T.; Koron, N.; Guevara, S.R.; Begu, E.; Barkay, T.; Horvat, M.; Falnoga, I.; Faganeli, J. Mercury transformations in a coastal water column (gulf of Trieste, Northern Adriatic sea). *Mar. Chem.* **2018**, *200*, 57–67. [CrossRef]